

## **Nuclear Waste and Biocatalysis**

### **A Sustainable Liaison?**

Zhang, Wuyuan; Liu, Huanhuan; Van Schie, Morten M.C.H.; Hagedoorn, Peter Leon; Alcalde, Miguel; Denkova, Antonia G.; Djanashvili, Kristina; Hollmann, Frank

**DOI**

[10.1021/acscatal.0c03059](https://doi.org/10.1021/acscatal.0c03059)

**Publication date**

2020

**Document Version**

Final published version

**Published in**

ACS Catalysis

**Citation (APA)**

Zhang, W., Liu, H., Van Schie, M. M. C. H., Hagedoorn, P. L., Alcalde, M., Denkova, A. G., Djanashvili, K., & Hollmann, F. (2020). Nuclear Waste and Biocatalysis: A Sustainable Liaison? *ACS Catalysis*, *10*(23), 14195-14200. <https://doi.org/10.1021/acscatal.0c03059>

**Important note**

To cite this publication, please use the final published version (if applicable).  
Please check the document version above.

**Copyright**

Other than for strictly personal use, it is not permitted to download, forward or distribute the text or part of it, without the consent of the author(s) and/or copyright holder(s), unless the work is under an open content license such as Creative Commons.

**Takedown policy**

Please contact us and provide details if you believe this document breaches copyrights.  
We will remove access to the work immediately and investigate your claim.

# Nuclear Waste and Biocatalysis: A Sustainable Liaison?

Wuyuan Zhang,\* Huanhuan Liu, Morten M. C. H. van Schie, Peter-Leon Hagedoorn, Miguel Alcalde, Antonia G. Denkova, Kristina Djanashvili, and Frank Hollmann\*



Cite This: *ACS Catal.* 2020, 10, 14195–14200



Read Online

ACCESS |



Metrics & More



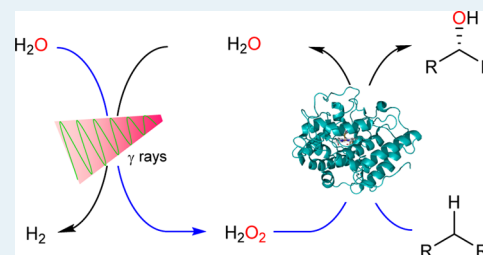
Article Recommendations



Supporting Information

**ABSTRACT:** It is well-known that energy-rich radiation induces water splitting, eventually yielding hydrogen peroxide. Synthetic applications, however, are scarce and to the best of our knowledge, the combination of radioactivity with enzyme-catalysis has not been considered yet. Peroxygenases utilize  $\text{H}_2\text{O}_2$  as an oxidant to promote highly selective oxyfunctionalization reactions but are also irreversibly inactivated in the presence of too high  $\text{H}_2\text{O}_2$  concentrations. Therefore, there is a need for efficient in situ  $\text{H}_2\text{O}_2$  generation methods. Here, we show that radiolytic water splitting can be used to promote specific biocatalytic oxyfunctionalization reactions. Parameters influencing the efficiency of the reaction and current limitations are shown. Particularly, oxidative inactivation of the biocatalyst by hydroxyl radicals influences the robustness of the overall reaction. Radical scavengers can alleviate this issue, but eventually, physical separation of the enzymes from the ionizing radiation will be necessary to achieve robust reaction schemes. We demonstrate that nuclear waste can also be used to drive selective, peroxygenase-catalyzed oxyfunctionalization reactions, challenging our view on nuclear waste in terms of sustainability.

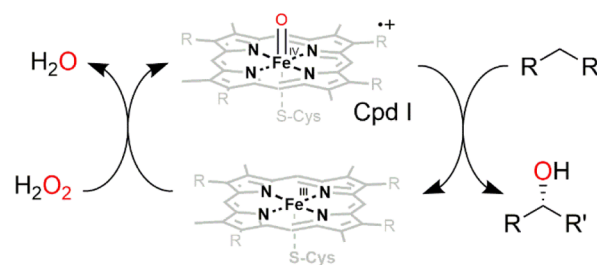
**KEYWORDS:** radiation, biocatalysis, oxyfunctionalization, peroxygenases, sustainability



It is known since decades that radiolytic splitting of water results in the formation of various radicals, which eventually form  $\text{H}_2\text{O}_2$  and  $\text{H}_2$ .<sup>1</sup> Interestingly, with the exception of radical-initiated polymerization of vinyl monomers<sup>2,3</sup> or hydrogen production,<sup>4</sup> this reaction has not yet caught the attention of organic chemists. Particularly, hydrogen peroxide could be used to drive a broad range of catalytic oxidation reactions.<sup>5</sup> Peroxygenases (UPOs, E.C. 1.11.2.1), for example, are a class of enzymes catalyzing a broad range of specific,  $\text{H}_2\text{O}_2$ -dependent oxyfunctionalization reactions ranging from the hydroxylation of aromatic and aliphatic C–H-bonds, epoxidation of C=C-bonds, and oxygenation of heteroatoms.<sup>6–8</sup> For this, peroxygenases utilize a heme prosthetic group, which in the presence of  $\text{H}_2\text{O}_2$  is transformed into an oxo-ferryl species (Compound I) mediating the oxyfunctionalization reaction (Scheme 1).<sup>7</sup> Utilizing this “ $\text{H}_2\text{O}_2$  shunt pathway”, peroxygenases are independent from the complex electron transport chains utilized by P450 monooxygenases to form Cpd I via reductive activation of  $\text{O}_2$ .<sup>9–12</sup>

In the presence of too high concentrations of  $\text{H}_2\text{O}_2$ , however, peroxygenases are also irreversibly inactivated.<sup>13–15</sup> To alleviate this issue, a range of in situ  $\text{H}_2\text{O}_2$  generation systems have been developed, mostly comprising catalytic reduction of  $\text{H}_2\text{O}_2$ .<sup>13</sup> These systems can be categorized by the sacrificial reductant used (Table S1). The well-known glucose oxidase system,<sup>16,17</sup> for example, transforms glucose into gluconic acid, thereby yielding more than 190 g of waste per mol  $\text{H}_2\text{O}_2$  generated. Formic acid,<sup>18</sup> methanol,<sup>19–21</sup>  $\text{H}_2$ ,<sup>22</sup> or electrochemical power<sup>23–26</sup> are more attractive from the atom

**Scheme 1. Peroxygenase Mechanism in a Nutshell; the Resting  $\text{Fe}^{\text{III}}$ –Heme Prosthetic Group Reacts with  $\text{H}_2\text{O}_2$  to Form Compound I (Cpd I,  $\text{Fe}^{\text{IV}}\text{Oxo}$ –Heme Radical Cation); the Latter can Insert the Activated O Atom Into C–H Bonds<sup>7</sup>**

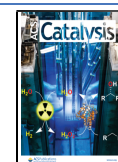


economy point of view. Water oxidation<sup>27–29</sup> appears most appealing as here, the atom efficiency is the highest. In this context, the radiolytic formation of  $\text{H}_2\text{O}_2$  may represent an interesting alternative method (Figure 1a).

Received: July 14, 2020

Revised: October 27, 2020

Published: November 20, 2020



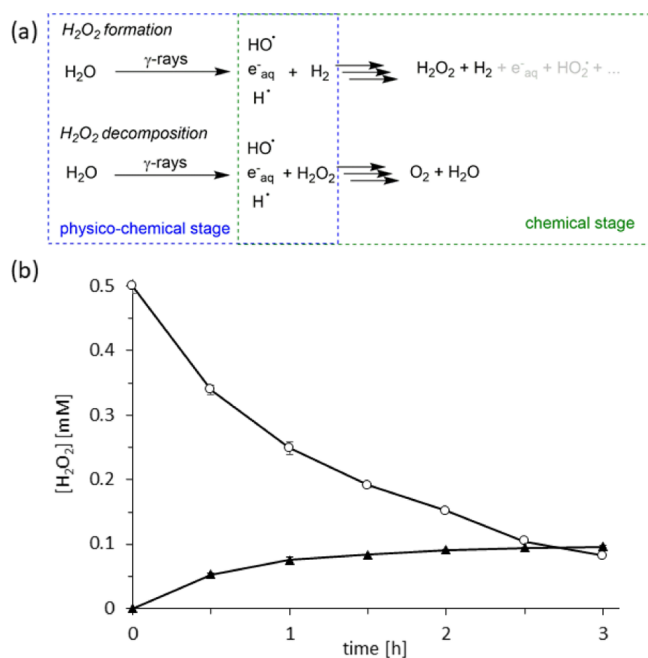


**Figure 1.** Radiolytic H<sub>2</sub>O<sub>2</sub> formation. (a) Schematic physicochemical and chemical steps involved in radiolytic H<sub>2</sub>O<sub>2</sub> formation and H<sub>2</sub>O<sub>2</sub> decomposition;<sup>30</sup> (b) H<sub>2</sub>O<sub>2</sub> concentration in aqueous phosphate buffer (100 mM, pH 7, *T* = 22 °C) exposed to a <sup>60</sup>Co-radiolysis source (12.9 Gy min<sup>-1</sup>). (▲): [H<sub>2</sub>O<sub>2</sub>]<sub>0</sub> = 0 mM, (○): [H<sub>2</sub>O<sub>2</sub>]<sub>0</sub> = 0.5 mM. Error bars indicate the standard deviation of duplicate experiments (*n* = 2).

As a radiation source, we used an external gamma radiation source <sup>60</sup>Co, which is widely applied, for example, in radiotherapy (i.e., gamma knife) and sterilization.

Indeed, an aqueous buffer placed next to the radiation source steadily accumulated H<sub>2</sub>O<sub>2</sub> up to 0.1 mM at which the H<sub>2</sub>O<sub>2</sub> concentration plateaued (in the case of a dose rate of 12.9 Gy min<sup>-1</sup>) (Figure 1b). In another experiment, we presupplemented the buffer with 0.5 mM H<sub>2</sub>O<sub>2</sub> and observed a steady decrease in the H<sub>2</sub>O<sub>2</sub> concentration to approximately 0.1 mM (Figure 1b). Apparently, the constant H<sub>2</sub>O<sub>2</sub> concentration was the result of a steady state between H<sub>2</sub>O splitting (yielding H<sub>2</sub>O<sub>2</sub>) and radiolysis-based splitting of H<sub>2</sub>O<sub>2</sub> (yielding H<sub>2</sub>O and O<sub>2</sub>).<sup>31</sup> The position of the steady state depended on the intensity (i.e., dose rate) of the radiation source (Figure S1).

Next, we combined the <sup>60</sup>Co-induced water radiolysis with a UPO-catalyzed hydroxylation reaction. As a model reaction, we used the selective hydroxylation of ethyl benzene to (*R*)-1-phenyl ethanol catalyzed by the recombinant, evolved peroxygenase from *Agroclybe aegerita* (rAaeUPO).<sup>32–34</sup> To confirm that the overall reaction followed the mechanism outlined in Figure 2a, a range of control reactions were executed: performing the reaction either in the absence or using thermally inactivated rAaeUPO yielded no product formation, while in the presence of rAaeUPO, enantiomerically pure (>99% ee) (*R*)-1-phenyl ethanol was formed. The presence or absence of molecular oxygen had no obvious influence on the product formation rate. Furthermore, performing the reaction in H<sub>2</sub><sup>18</sup>O-enriched buffer resulted in the formation of <sup>18</sup>O-labeled (*R*)-1-phenyl ethanol (Figure 2b,c). This confirms that indeed the reaction medium serves as a source of H<sub>2</sub>O<sub>2</sub> and that reduction of O<sub>2</sub> (from ambient air) played a minor role in the H<sub>2</sub>O<sub>2</sub> formation.

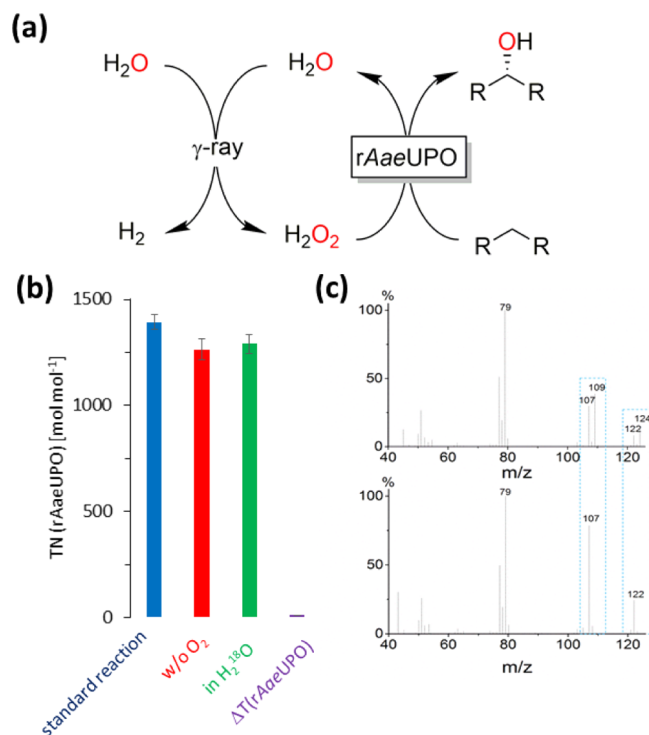


**Figure 2.** Selective hydroxylation of ethyl benzene to (*R*)-1-phenyl ethanol using rAaeUPO and radiolysis-derived H<sub>2</sub>O<sub>2</sub>: (a) reaction scheme; (b) turnover numbers (TN = moles<sub>(*R*)-1-phenyl ethanol</sub> × moles<sub>rAaeUPO</sub><sup>-1</sup>): (blue): standard reaction ([rAaeUPO] = 200 nM, [substrate] = 5 mM); (red): w/o O<sub>2</sub> (using deaerated reaction mixtures); (green): in H<sub>2</sub><sup>18</sup>O (under aerobic conditions but using <sup>18</sup>O-enriched water); (violet): ΔT(rAaeUPO) (using a thermally inactivated biocatalyst); (c) GC/MS analysis of the reaction product ((*R*)-1-phenyl ethanol) obtained from the reaction in <sup>18</sup>O-enriched water (upper) and under standard conditions (lower). Error bars indicate the standard deviation of duplicate experiments (*n* = 2).

(*R*)-1-phenyl ethanol was the sole product observed, indicating that the selectivity of the biocatalyst was not impaired under the reaction conditions, particularly by the radioactivity. A control reaction with (*R*)-1-phenyl ethanol only under the irradiation showed that radiation-induced further oxidation of the primary enzyme product ((*R*)-1-phenyl ethanol to acetophenone) can be ruled out.

Next, we further investigated some factors influencing the efficiency and robustness of the overall reaction (Figure 3). Increasing the biocatalyst concentration increased the product formation within the first hour (Figure 3a). This increase, however, was not linear and converged to approx. 0.25 mM h<sup>-1</sup> at rAaeUPO concentrations above 100 nM. Interestingly, this product formation rate was approx. twofold higher than the H<sub>2</sub>O<sub>2</sub> accumulation rate observed in the absence of the biocatalysts (Figure 1b). This observation can be attributed to the irreversible peroxygenase step removing H<sub>2</sub>O<sub>2</sub> from the steady-state equilibrium. A respectable turnover number for the biocatalyst (TN = moles<sub>Product</sub> × moles<sub>Catalyst</sub><sup>-1</sup>) of more than 1400 was observed for the biocatalyst.

These experiments, however, also revealed a poor long-term stability of the enzyme under the reaction conditions. Already after 1 h of reaction (approx. 770 Gy under the dose rate of 12.9 Gy min<sup>-1</sup>), the product formation ceased, which we interpreted as loss of enzyme activity (Figure S2). This assumption is supported by a considerable decrease in the

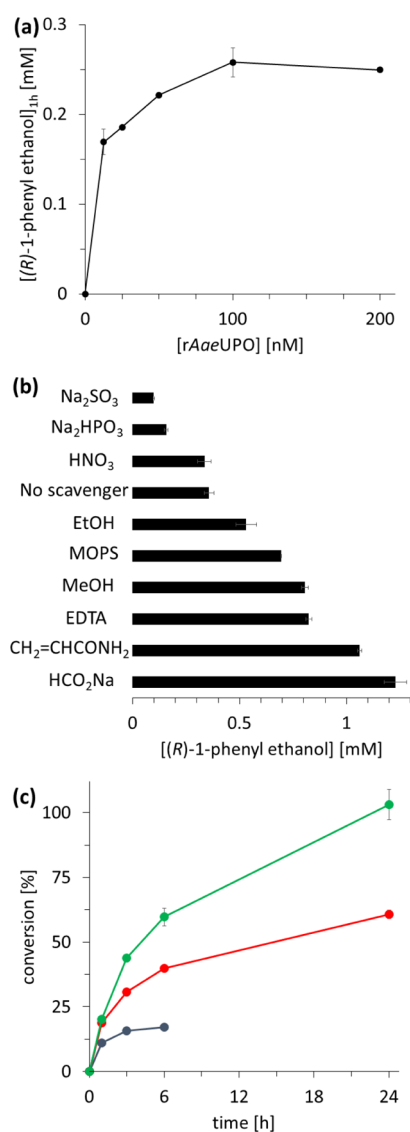


**Figure 3.** (a) Influence of the biocatalyst concentration on the “initial” product formation within the first hour of reaction; (b) influence of various radical scavenger molecules (50 mM each) on the product formation after 1 h reaction time; (c) comparison of the time courses of the radioenzymatic hydroxylation in the absence of radical scavengers (blue ●) or in the presence of methanol (red ●, 50 mM) or sodium formate (green ●, 50 mM). Reaction conditions: [substrate] = 2 mM, [rAaeUPO] = 50 nM (b,c), NaPi, pH 7.0 (60 mM),  $T = 22\text{ }^{\circ}\text{C}$ ,  $t = 1\text{ h}$  (a,b). The dose rate was  $12.9\text{ Gy min}^{-1}$ . Error bars indicate the standard deviation of duplicate experiments ( $n = 2$ ).

characteristic Soret peak at 419 nm indicative for an intact heme moiety (Figure S3). Analysis of an inactivated enzyme sample by native gel electrophoresis gave no indication for loss of the quaternary structure (Figure S4). We reasoned that hydroxyl radicals formed during the physicochemical phase of the water radiolysis reaction, for example, the hydroxyl radicals, may oxidatively inactivate the catalytic heme functionality and thereby the biocatalyst. Of course, also  $\text{H}_2\text{O}_2$ -dependent inactivation of the prosthetic group can also contribute to the observed inactivation. However, also the highly  $\text{H}_2\text{O}_2$ -stable,<sup>35</sup> V-dependent chloroperoxidase from *Curvularia inaequalis* (CiVCP)<sup>36</sup> was inactivated under these conditions (vide infra). Suspecting intermediate radical species (Figure

1a) as major contributors to the observed biocatalyst inactivation, we tested a range of different radical scavengers (Figure 3b). Among these radical scavengers especially methanol, acrylamide, and formate enabled significantly increased product formation (Figure 3b). The effect depended on the concentration of the radical scavenger as exemplified with methanol and formate (Figures S5 and S6). We therefore also compared the time courses of the radioenzymatic reactions in the absence and presence of the radical scavengers methanol and formate (Figure 3c). Most strikingly, the conversion of ethyl benzene to (R)-1-phenyl ethanol was increased from approx. 18%, in the case of reactions in the absence of radical scavengers, to full conversion, in the presence of sodium formate. In the latter case, a turnover number for the biocatalyst of 40,000 was achieved, which we ascribe to a higher enzyme stability because of a decreased concentration of hydroxyl radicals. This assumption was also supported by electron paramagnetic resonance experiments, which revealed that in the presence of both methanol or formate, the in situ  $\cdot\text{OH}$  concentration was significantly reduced (Figures S7 and S8).

The dose rate of the radiation source directly influenced the product formation of the radioenzymatic reaction system (Table 1). The final product concentration (and directly

**Table 1.** Radioenzymatic Hydroxylation of Ethyl Benzene Using Different Radiation Sources<sup>a</sup>

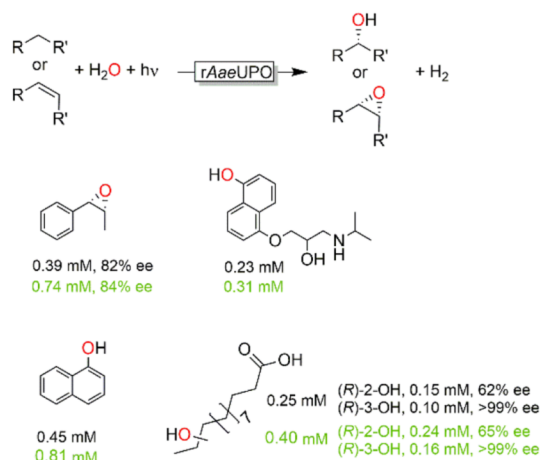
radiation source <sup>b</sup>	<sup>60</sup> Co-1	<sup>60</sup> Co-2	<sup>235</sup> U
dose rate [ $\text{Gy min}^{-1}$ ]	12.9	1.0	1.67
(R)-1-phenyl ethanol [mM]	0.91	0.29	0.39
ee [%]	>99	>99	>99
$\text{TON}_{\text{rAaeUPO}}^c$	18,200	5800	7800
radiation yield [ $\mu\text{M}_{\text{product}} \times \text{Gy}^{-1}$ ] <sup>d</sup>	0.196	0.806	0.659

<sup>a</sup>General reaction conditions: sodium phosphate buffer (60 mM, pH 7), [ethyl benzene] = 1 mM, [rAaeUPO] = 50 nM, [sodium formate] = 50 mM,  $T = 22\text{ }^{\circ}\text{C}$ ,  $t = 6\text{ h}$ . <sup>b</sup>Three different radiation sources were used: <sup>60</sup>Co-1 and -2 exhibiting dose rates of 12.9 and 1  $\text{Gy min}^{-1}$ , respectively, and <sup>235</sup>U (from a spent fuel element) with 1.67  $\text{Gy min}^{-1}$ . <sup>c</sup> $\text{TON}_{\text{rAaeUPO}} = \text{moles}_{\text{product}} \times \text{moles}_{\text{rAaeUPO}}^{-1}$ . <sup>d</sup>Radiation yield = product concentration  $\times$  (dose rate  $\times$  reaction time)<sup>-1</sup>.

related to this also the turnover number of the enzyme) directly correlated with the dose rate of the radioactivity source applied. Interestingly, the “radiation yield”, that is, the amount of product formed per Gy, correlated inversely with the dose rate. This may be due to a decreased radiolytic  $\text{H}_2\text{O}_2$  decomposition at lower dose rates, whereas the biocatalyst concentration remained constant. Further experiments will be necessary to fully rationalize this observation. Pleasantly, the reactions performed with spent fuel element (<sup>235</sup>U) also showed good robustness.

Finally, we initially explored the substrate scope of the proposed radioenzymatic reaction scheme (Figure 4). For this, some further oxyfunctionalization reactions reported for rAaeUPO, such as epoxidation<sup>37</sup> as well as aliphatic<sup>38</sup> and aromatic hydroxylation reactions, were chosen.<sup>39,40</sup> With the exception of the epoxidation of *cis*- $\beta$ -methyl styrene, where the optical purity of the epoxide product was somewhat lower than reported, the regio- and enantioselectivity of the biocatalyst was not impaired under the reaction conditions and essentially identical results compared to previous experiments with this enzyme using alternative  $\text{H}_2\text{O}_2$  generation methods were

## a) rAaeUPO-catalyzed oxyfunctionalization reactions



## b) CiVCPO-catalyzed hydroxybromination reactions



**Figure 4.** Preliminary product scope of the proposed radioenzymatic reactions. (a) Specific oxyfunctionalization reactions catalyzed by rAaeUPO; (b) CiVCPO-catalyzed hydroxybromination reactions. Reaction results shown in black originate from reactions in the absence of formate, whereas results shown in green stem from reactions performed (under otherwise identical conditions) in the presence of 50 mM NaHCO<sub>2</sub>. Reaction conditions: General: the dose rate in each experiment was 12.9 Gy min<sup>-1</sup>, T = 22 °C, t = 6 h, experiments were performed as duplicates; (a) [substrate] = 1 mM, buffer: NaPi buffer (50 mM, pH 7) except for the reaction of tridecanoic acid (50 mM Tris-HCl, pH 8), 30% (v/v) MeCN as cosolvent, [rAaeUPO] = 50 nM, (b) [substrate] = 1 mM, buffer: citrate buffer (100 mM, pH 5), [CiVCPO] = 50 nM, [NaBr] = 5 mM.

observed. Possibly, the radicals present in the reaction mixture lead to racemization of the epoxide product, but further investigations will be necessary to confirm this. Again, a beneficial effect of formate on the product formation was observed (Figure 4).

To address the question whether too high H<sub>2</sub>O<sub>2</sub> concentrations may contribute to the abovementioned inactivation of rAaeUPO, we extended the enzyme scope of the proposed radioenzymatic reaction to the vanadium-dependent chloroperoxidase from *C. inaequalis* (CiVCPO).<sup>36</sup> CiVCPO exhibits superb stability even in the presence of up to 100 mM.<sup>35</sup> Using CiVCPO as a catalyst to the hydroxybromination of styrene<sup>41</sup> and the bromolactonization of 4-pentenoic acid,<sup>42,43</sup> significant product accumulation was observed. The turnover numbers achieved for the biocatalyst (>4000), however, fell back behind the numbers observed previously. As H<sub>2</sub>O<sub>2</sub> as a cause for this can be ruled out, we assign this observation to CiVCPO inactivation by hydroxyl radicals (Figure S9).

In conclusion, we have demonstrated that radiolytic water splitting can be used to promote biocatalytic oxyfunctionalization reactions. H<sub>2</sub>O<sub>2</sub> formed as a consequence of  $\gamma$ -irradiation of the reaction mixture enabled “donor-independent” H<sub>2</sub>O<sub>2</sub> generation from water. The dose-rate-dependent steady-state

concentration appears ideal to provide heme-dependent peroxygenases with suitable concentrations of H<sub>2</sub>O<sub>2</sub> that enable the reaction while minimizing the oxidative inactivation. This advantage, at least in the present setup, is compensated by the radical-induced inactivation of the biocatalyst, this is also reflected by the comparably poor performance of the present system compared to other in situ H<sub>2</sub>O<sub>2</sub> generation systems (Table S1). Compared with (enzymatic) H<sub>2</sub>O<sub>2</sub> generation systems (which largely avoid the intermediate occurrence of radical species), the peroxygenases’ turnover numbers fall back approx. 10-fold. Compared to other (radical-generating) H<sub>2</sub>O<sub>2</sub> generation systems, the turnover numbers observed here compare very well. The radical inactivation of the biocatalysts represents an apparent shortcoming of the current setup. In future experiments, we will address this by physical separation of the biocatalyst from the radiation source. Flow chemistry appears a particularly attractive technical solution.

Although this approach at first sight may appear as a lab curiosity, we believe that it may actually bear some practical relevance. In this study, we have demonstrated that spent fuel elements can drive peroxygenase-catalyzed reactions. Considering the annually increasing amounts of radioactive waste and its persistence, the proposed radioenzymatic approach may represent a possibility to productively utilize nuclear waste. Furthermore, it should be kept in mind that globally a variety of different radiation sources are used commercially. For instance, <sup>60</sup>Co units are used for sterilization and electron beams for various applications and research nuclear reactors (more than 250 worldwide).

## EXPERIMENTAL SECTION

**Production of the Biocatalysts.** The evolved, unspecific peroxygenase from *Agrocybe aegrita* (rAaeUPO) was obtained from fermentation of recombinant *Pichia pastoris* as previously described.<sup>33,34</sup> The culture broth containing rAaeUPO in the supernatant was clarified by centrifugation followed by ultrafiltration and filtered through a 20  $\mu$ m filter. The enzyme preparation was stored at -80 °C until further use. The vanadium-dependent chloroperoxidase from *C. inaequalis* (CiVCPO) was produced by recombinant expression in *Escherichia coli* as described previously.<sup>35</sup> The crude cell extracts were treated with isopropanol (50% v/v) to precipitate nucleic acids and endogenous *E. coli* proteins. The clarified supernatant was supplemented with (NH<sub>4</sub>)<sub>2</sub>VO<sub>4</sub> (100  $\mu$ M<sub>final</sub>) to reconstitute the holoenzyme.

**Radiochemical Experiments.** All radiochemical experiments were performed by placing 2 mL GC vials filled with 1 mL of the reaction mixture next to the radioactivity source (Figure S10). All reactions were performed at ambient temperature (22 °C). At intervals, samples were removed from the radiation source and analyzed. For H<sub>2</sub>O<sub>2</sub> quantification, we used using Ghormley’s triiodide method.<sup>44</sup> For the analysis of the radioenzymatic reactions, the reaction mixtures were further processed and analyzed by GC or HPLC as described previously.<sup>21,45,46</sup>

## ASSOCIATED CONTENT

### Supporting Information

The Supporting Information is available free of charge at <https://pubs.acs.org/doi/10.1021/acscatal.0c03059>.

Detailed experimental and analytical details and further experimental results (PDF)

## AUTHOR INFORMATION

## Corresponding Authors

Wuyuan Zhang – Department of Biotechnology, Delft University of Technology, 2629 HZ Delft, The Netherlands; Tianjin Institute of Industrial Biotechnology, Chinese Academy of Sciences, 300308 Tianjin, China; [orcid.org/0000-0002-3182-5107](https://orcid.org/0000-0002-3182-5107); Email: [zhangwy@tib.cas.cn](mailto:zhangwy@tib.cas.cn)

Frank Hollmann – Department of Biotechnology, Delft University of Technology, 2629 HZ Delft, The Netherlands; [orcid.org/0000-0003-4821-756X](https://orcid.org/0000-0003-4821-756X); Email: [f.hollmann@tudelft.nl](mailto:f.hollmann@tudelft.nl)

## Authors

Huanhuan Liu – Radiation Science and Technology, Delft University of Technology, 2629 JB Delft, The Netherlands

Morten M. C. H. van Schie – Department of Biotechnology, Delft University of Technology, 2629 HZ Delft, The Netherlands

Peter-Leon Hagedoorn – Department of Biotechnology, Delft University of Technology, 2629 HZ Delft, The Netherlands; [orcid.org/0000-0001-6342-2022](https://orcid.org/0000-0001-6342-2022)

Miguel Alcalde – Department of Biocatalysis, Institute of Catalysis, CSIC, 28049 Madrid, Spain; [orcid.org/0000-0001-6780-7616](https://orcid.org/0000-0001-6780-7616)

Antonia G. Denkova – Radiation Science and Technology, Delft University of Technology, 2629 JB Delft, The Netherlands

Kristina Djanashvili – Department of Biotechnology, Delft University of Technology, 2629 HZ Delft, The Netherlands; [orcid.org/0000-0003-1511-015X](https://orcid.org/0000-0003-1511-015X)

Complete contact information is available at: <https://pubs.acs.org/10.1021/acscatal.0c03059>

## Notes

The authors declare no competing financial interest.

## ACKNOWLEDGMENTS

Financial support by the European Research Council (ERC Consolidator Grant no. 648026) is gratefully acknowledged. W.Z. gratefully acknowledges financial support by Tianjin Institute of Industrial Biotechnology, Chinese Academy of Sciences. We thank Astrid van de Meer for excellent technical assistance with  $^{60}\text{Co}$  irradiation.

## REFERENCES

- (1) Le Caër, S. Water Radiolysis: Influence of Oxide Surfaces on  $\text{H}_2$  Production under Ionizing Radiation. *Water* **2011**, *3*, 235–253.
- (2) Yao, T.; Denkova, A. G.; Warman, J. M. Polymer-gel formation and reformation on irradiation of tertiary-butyl acrylate. *Rad. Phys. Chem.* **2014**, *97*, 147–152.
- (3) Chen, C. S. H.; Stamm, R. F. Polymerization induced by ionizing radiation at low temperatures. I. Evidence for the simultaneous existence of ionic and free-radical mechanisms in the polymerization of styrene and 2,4-dimethylstyrene. *J. Polym. Sci.* **1962**, *58*, 369–388.
- (4) Kumagai, Y.; Kimura, A.; Taguchi, M.; Watanabe, M. Hydrogen Production by  $\gamma$ -Ray Irradiation from Different Types of Zeolites in Aqueous Solution. *J. Phys. Chem. C* **2017**, *121*, 18525–18533.
- (5) Noyori, R.; Aoki, M.; Sato, K. Green oxidation with aqueous hydrogen peroxide. *Chem. Commun.* **2003**, 1977–1986.
- (6) Wang, Y.; Lan, D.; Durrani, R.; Hollmann, F. Peroxygenases en route to becoming dream catalysts. What are the opportunities and challenges? *Curr. Opin. Chem. Biol.* **2017**, *37*, 1–9.
- (7) Hofrichter, M.; Ullrich, R. Oxidations catalyzed by fungal peroxygenases. *Curr. Opin. Chem. Biol.* **2014**, *19*, 116–125.

(8) Hobisch, M.; Holtmann, D.; Gomez de Santos, P.; Alcalde, M.; Hollmann, F.; Kara, S. Recent developments in the use of peroxygenases – Exploring their high potential in selective oxyfunctionalisations. *Biotechnol. Adv.* **2020**, 107615.

(9) Urlacher, V. B.; Girhard, M. Cytochrome P450 Monooxygenases in Biotechnology and Synthetic Biology. *Trends Biotechnol.* **2019**, *37*, 882–897.

(10) Glieder, A.; Farinas, E. T.; Arnold, F. H. Laboratory evolution of a soluble, self-sufficient, highly active alkane hydroxylase. *Nat. Biotechnol.* **2002**, *20*, 1135–1139.

(11) Joo, H.; Lin, Z.; Arnold, F. H. Laboratory evolution of peroxide-mediated cytochrome P450 hydroxylation. *Nature* **1999**, *399*, 670–673.

(12) Fasan, R. Tuning P450 Enzymes as Oxidation Catalysts. *ACS Catal.* **2012**, *2*, 647–666.

(13) Burek, B. O.; Bormann, S.; Hollmann, F.; Bloh, J. Z.; Holtmann, D. Hydrogen peroxide driven biocatalysis. *Green Chem.* **2019**, *21*, 3232–3249.

(14) Ayala, M.; Batista, C. V.; Vazquez-Duhalt, R. Heme destruction, the main molecular event during the peroxide-mediated inactivation of chloroperoxidase from *Caldariomyces fumago*. *J. Biol. Inorg. Chem.* **2011**, *16*, 63–68.

(15) Valderrama, B.; Ayala, M.; Vazquez-Duhalt, R. Suicide Inactivation of Peroxidases and the Challenge of Engineering More Robust Enzymes. *Chem. Biol.* **2002**, *9*, 555–565.

(16) Pereira, P. C.; Arends, I. W. C. E.; Sheldon, R. A. Optimizing the chloroperoxidase-glucose oxidase system: The effect of glucose oxidase on activity and enantioselectivity. *Proc. Biochem.* **2015**, *50*, 746–751.

(17) van Rantwijk, F.; Sheldon, R. A. Selective oxygen transfer catalysed by heme peroxidases: synthetic and mechanistic aspects. *Curr. Opin. Biotechnol.* **2000**, *11*, 554–564.

(18) Tieves, F.; Willot, S. J. P.; van Schie, M. M. C. H.; Rauch, M. C. R.; Younes, S. H. H.; Zhang, W.; Dong, J.; Gomez de Santos, P.; Robbins, J. M.; Bommarius, B.; Alcalde, M.; Bommarius, A. S.; Hollmann, F. Formate oxidase (FOx) from *Aspergillus oryzae*: one catalyst to promote  $\text{H}_2\text{O}_2$ -dependent biocatalytic oxidation reactions. *Angew. Chem., Int. Ed.* **2019**, *58*, 7873–7877.

(19) Willot, S. J. P.; Hoang, M. D.; Paul, C. E.; Alcalde, M.; Arends, I. W. C. E.; Bommarius, A. S.; Bommarius, B.; Hollmann, F. FOx News: Towards Methanol-driven Biocatalytic Oxyfunctionalisation Reactions. *ChemCatChem* **2020**, *12*, 2713–2716.

(20) Zhang, W.; Burek, B. O.; Fernández-Fueyo, E.; Alcalde, M.; Bloh, J. Z.; Hollmann, F. Selective activation of C-H bonds by cascading photochemistry with biocatalysis. *Angew. Chem., Int. Ed.* **2017**, *56*, 15451–15455.

(21) Ni, Y.; Fernández-Fueyo, E.; Baraibar, A. G.; Ullrich, R.; Hofrichter, M.; Yanase, H.; Alcalde, M.; van Berkel, W. J. H.; Hollmann, F. Peroxygenase-catalyzed oxyfunctionalization reactions promoted by the complete oxidation of methanol. *Angew. Chem., Int. Ed.* **2016**, *55*, 798–801.

(22) Al-Shameri, A.; Willot, S. J.-P.; Paul, C. E.; Hollmann, F.; Lauterbach, L.  $\text{H}_2$  as a fuel for flavin- and  $\text{H}_2\text{O}_2$ -dependent biocatalytic reactions. *Chem. Commun.* **2020**, 9667–9670.

(23) Bormann, S.; Schie, M. M. C. H.; De Almeida, T. P.; Zhang, W.; Stöckl, M.; Ulber, R.; Hollmann, F.; Holtmann, D.  $\text{H}_2\text{O}_2$  Production at Low Overpotentials for Electroenzymatic Halogenation Reactions. *ChemSusChem* **2019**, *12*, 4759–4763.

(24) Horst, A. E. W.; Bormann, S.; Meyer, J.; Steinhagen, M.; Ludwig, R.; Drews, A.; Ansoorge-Schumacher, M.; Holtmann, D. Electro-enzymatic hydroxylation of ethylbenzene by the evolved unspecific peroxygenase of *Agroclybe aegerita*. *J. Mol. Catal. B: Enzym.* **2016**, *133*, S137–S142.

(25) Getrey, L.; Krieg, T.; Hollmann, F.; Schrader, J.; Holtmann, D. Enzymatic halogenation of the phenolic monoterpenes thymol and carvacrol with chloroperoxidase. *Green Chem.* **2014**, *16*, 1104–1108.

(26) Lütz, S.; Steckhan, E.; Liese, A. First asymmetric electro-enzymatic oxidation catalyzed by a peroxidase. *Electrochem. Commun.* **2004**, *6*, 583–587.

- (27) Yoon, J.; Kim, J.; Tieves, F.; Zhang, W.; Alcalde, M.; Hollmann, F.; Park, C. B. Piezobiocatalysis: Ultrasound-Driven Enzymatic Oxyfunctionalization of C-H Bonds. *ACS Catal.* **2020**, *10*, 5236–5242.
- (28) Zhang, W.; Fernández-Fueyo, E.; Ni, Y.; van Schie, M.; Gacs, J.; Renirie, R.; Wever, R.; Mutti, F. G.; Rother, D.; Alcalde, M.; Hollmann, F. Selective aerobic oxidation reactions using a combination of photocatalytic water oxidation and enzymatic oxyfunctionalizations. *Nat. Catal.* **2018**, *1*, 55–62.
- (29) Yayci, A.; Baraibar, Á. G.; Krewing, M.; Fueyo, E. F.; Hollmann, F.; Alcalde, M.; Kourist, R.; Bandow, J. E. Plasma-Driven in Situ Production of Hydrogen Peroxide for Biocatalysis. *ChemSusChem* **2020**, *13*, 2072–2079.
- (30) Iwamatsu, K.; Sundin, S.; LaVerne, J. A. Hydrogen peroxide kinetics in water radiolysis. *Rad. Phys. Chem.* **2018**, *145*, 207–212.
- (31) Joseph, J. M.; Seon Choi, B.; Yakabuskie, P.; Clara Wren, J. A combined experimental and model analysis on the effect of pH and O<sub>2</sub>(aq) on  $\gamma$ -radiolytically produced H<sub>2</sub> and H<sub>2</sub>O<sub>2</sub>. *Rad. Phys. Chem.* **2008**, *77*, 1009–1020.
- (32) Ullrich, R.; Nüske, J.; Scheibner, K.; Spantzel, J.; Hofrichter, M. Novel haloperoxidase from the agaric basidiomycete *Agrocybe aegerita* oxidizes aryl alcohols and aldehydes. *Appl. Environ. Microbiol.* **2004**, *70*, 4575–4581.
- (33) Molina-Espeja, P.; Ma, S.; Mate, D. M.; Ludwig, R.; Alcalde, M. Tandem-yeast expression system for engineering and producing unspecific peroxygenase. *Enzyme Microb. Technol.* **2015**, *73–74*, 29–33.
- (34) Molina-Espeja, P.; Garcia-Ruiz, E.; Gonzalez-Perez, D.; Ullrich, R.; Hofrichter, M.; Alcalde, M. Directed Evolution of Unspecific Peroxygenase from *Agrocybe aegerita*. *Appl. Environ. Microbiol.* **2014**, *80*, 3496–3507.
- (35) Fernández-Fueyo, E.; van Wingerden, M.; Renirie, R.; Wever, R.; Ni, Y.; Holtmann, D.; Hollmann, F. Chemoenzymatic halogenation of phenols by using the haloperoxidase from *Curvularia inaequalis*. *ChemCatChem* **2015**, *7*, 4035–4038.
- (36) van Schijndel, J. W. P. M.; Vollenbroek, E. G. M.; Wever, R. The chloroperoxidase from the fungus *Curvularia inaequalis* - a novel vanadium enzyme. *Biochim. Biophys. Acta* **1993**, *1161*, 249–256.
- (37) Kluge, M.; Ullrich, R.; Scheibner, K.; Hofrichter, M. Stereoselective benzylic hydroxylation of alkylbenzenes and epoxidation of styrene derivatives catalyzed by the peroxygenase of *Agrocybe aegerita*. *Green Chem.* **2012**, *14*, 440–446.
- (38) Gutiérrez, A.; Babot, E. D.; Ullrich, R.; Hofrichter, M.; Martínez, A. T.; del Río, J. C. Regioselective oxygenation of fatty acids, fatty alcohols and other aliphatic compounds by a basidiomycete heme-thiolate peroxidase. *Arch. Biochem. Biophys.* **2011**, *514*, 33–43.
- (39) Kinne, M.; Poraj-Kobielska, M.; Aranda, E.; Ullrich, R.; Hammel, K. E.; Scheibner, K.; Hofrichter, M. Regioselective preparation of 5-hydroxypropranolol and 4'-hydroxydiclofenac with a fungal peroxygenase. *Bioorg. Med. Chem. Lett.* **2009**, *19*, 3085–3087.
- (40) Kinne, M.; Ullrich, R.; Hammel, K. E.; Scheibner, K.; Hofrichter, M. Regioselective preparation of (R)-2-(4-hydroxyphenoxy)propionic acid with a fungal peroxygenase. *Tetrahedron Lett.* **2008**, *49*, 5950–5953.
- (41) Dong, J. J.; Fernández-Fueyo, E.; Li, J.; Guo, Z.; Renirie, R.; Wever, R.; Hollmann, F. Halofunctionalization of alkenes by vanadium chloroperoxidase from *Curvularia inaequalis*. *Chem. Commun.* **2017**, *53*, 6207–6210.
- (42) Younes, S. H. H.; Tieves, F.; Lan, D.; Wang, Y.; Süß, P.; Brundiek, H.; Wever, R.; Hollmann, F. Chemoenzymatic Halocyclization of gamma, delta-Unsaturated Carboxylic Acids and Alcohols. *ChemSusChem* **2020**, *13*, 97–101.
- (43) Höfler, G. T.; But, A.; Younes, S. H. H.; Wever, R.; Paul, C. E.; Arends, I. W. C. E.; Hollmann, F. Chemoenzymatic Halocyclization of 4-Pentenoic Acid at Preparative Scale. *ACS Sustainable Chem. Eng.* **2020**, *8*, 2602–2607.
- (44) Ghormley, J. A.; Stewart, A. C. Effects of  $\gamma$ -Radiation on Ice1. *J. Am. Chem. Soc.* **1956**, *78*, 2934–2939.
- (45) Rauch, M. C. R.; Tieves, F.; Paul, C. E.; Arends, I. W. C. E.; Alcalde, M.; Hollmann, F. Peroxygenase-catalysed epoxidation of styrene derivatives in neat reaction media. *ChemCatChem* **2019**, *11*, 4519–4523.
- (46) Gomez de Santos, P.; Cervantes, F. V.; Tieves, F.; Plou, F. J.; Hollmann, F.; Alcalde, M. Benchmarking of laboratory evolved unspecific peroxygenases for the synthesis of human drug metabolites. *Tetrahedron* **2019**, *75*, 1827–1831.